

# Stability design of long precast concrete beams

T. J. Stratford, BA, MEng, C. J. Burgoyne BA, MSc, CEng, MICE, and H. P. J. Taylor, BSc, PhD, FEng, FICE, FIStructE

Proc. Instn Civ. Engrs Structs & Bldgs, 1999, 134, May, 159–168

Paper 11808

Written discussion closes 27 August 1999

This paper presents the equations needed for design engineers to check the stability of precast concrete beams when simply supported, during transportation, when being lifted and while sitting on flexible bearings. It shows how the critical loads can be determined and how estimates can be made of the effect of imperfections both in the beam itself and in the degree of levelness of its supports. It shows how the stresses induced by second-order effects in imperfect beams can be determined. Various examples are given of the method in use.

**Keywords:** beams & girders; design methods & aids

## Notation

$A$	cross-sectional area
$a$	distance of yoke attachment point from end of beam
$b$	distance of yoke attachment point from centre of beam
$d$	beam depth
$E$	Young's modulus of concrete
$G$	shear modulus of concrete
$h$	height of yoke to cable attachment points above the centroid of the beam
$I_x$	second moment of area about the beam section's major axis
$I_y$	second moment of area about the beam section's minor axis
$J$	St Venant's torsion constant for beam section
$L$	length of beam
$v$	lateral deflection measured in the minor-axis direction (which rotates with $\theta$ )
$v_0$	initial lateral imperfection
$w$	self-weight of beam per unit length
$w_{cr}$	critical self-weight of beam to cause buckling, per unit length
$y$	lateral deflection measured along a fixed axis
$y_0$	initial lateral imperfection
$y_b$	distance of bottom fibre of beam below centroid of beam
$y_{ms}$	midspan lateral deflection measured along an axis fixed relative to the supports
$\alpha$	cable inclination angle above the horizontal
$\beta$	yoke inclination angle above the horizontal
	magnitude of initial lateral imperfection

$\eta$	rotation of supports giving rise to tilt of beam
$\theta$	roll angle: rigid-body rotation about the beam's axis
$\delta\theta$	twist about beam axis
$\kappa_{ms}$	midspan curvature about minor axis
$\mu$	axial load parameter in hanging-beam buckling analysis
$\sigma_y$	major-axis bending stress
$\Delta\sigma$	additional stress due to minor-axis buckling effects

## Introduction

The stability of precast prestressed concrete beams is becoming a cause for concern. If spans get longer and beams more slender, such beams are liable to buckle under their own self-weight at various stages in the manufacturing, handling and erection processes. The problem of a beam hanging from cables (as during lifting)<sup>1</sup> is the most severe case since there is no lateral restraint. A companion paper<sup>2</sup> gives a theoretical background to the general problem of lateral stability in various cases. This paper gives the information needed to incorporate stability criteria into the design of these beams. The intention is that this paper should be complete in its own right, but designers should familiarize themselves with the principles in the other two papers<sup>1,2</sup> if designs are being pushed to the limits imposed by the stability criteria.

2. The requirement for longer beams to span widened motorways led to the design first of the Y-beam<sup>3</sup> and subsequently the SY-beam,<sup>4</sup> which can span up to 40 m. These beams have to be deep to provide the required bending resistance about the major axis, but the weight has to be kept down for transportation reasons; they thus have only residual flanges. This gives them a relatively low minor-axis stiffness, which means that they could be susceptible to buckling before a top slab is cast.

3. It has been shown<sup>2</sup> that the largest SY-beam (the SY-6), when used at its maximum span, does not suffer from stability problems, but it is clear that any further increase in beam sizes would mean that stability considerations would have to be taken into account from the outset.

## Buckling phenomena

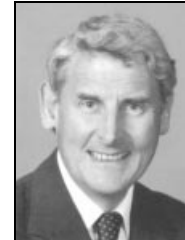
4. Three types of buckling failure of beams have been identified.<sup>2</sup> Unlike the case of steel



T. J. Stratford,  
Department of  
Engineering,  
University of  
Cambridge



C. J. Burgoyne,  
Department of  
Engineering,  
University of  
Cambridge



H. P. J. Taylor,  
Tarmac Building  
Products

beams, these buckling modes all relate to the beam acting under its own dead weight alone. It is assumed that the beam will be stabilized by a top slab or in some other way when subjected to a superimposed load. The three types of failure are as follows.

- (a) If a beam is simply supported on bearings which allow rotation about the major axis but are fixed about the minor axis, the beam can buckle to one side. Since the bearings restrain rotation at the supports, the buckling mode must involve twist as well as minor-axis bending, so a lateral-torsional buckle occurs. This will be called the *simply supported* case (Fig. 1(a)). Two types of initial imperfection need to be designed for: minor-axis beam deflection and rotation of the support.
- (b) When the beam is being transported, the arrangement of the supports and turntables on the truck and trailer means that a situation can occur where one end of the beam is not restrained against rotation (Fig. 1(b)). This will allow buckling to occur at a load lower than in the simply supported case; this situation will be termed the *transport-supported* case. As with the simply supported case, both minor-axis deflection and rotated-support imperfection conditions need to be allowed for.
- (c) The beam has to be lifted into position, which for long beams is normally carried out by two cranes acting in tandem, or by a single crane with or without a spreader beam (Fig. 1(c)). During this operation, the beam can twist as a rigid body, so that some of the beam's weight acts about the minor axis; large flexural deflections can occur without any variation of twist along the beam. Such deflections will be referred to as *toppling*. This will be termed the *hanging-beam* problem, and has been shown<sup>1,2</sup> to be the most critical of the three cases. Although only one initial imperfection has to be considered (lateral deflection), different equations have to be used depending on whether the cables are vertical or inclined.

5. A fourth case, associated with rotation about the beam's long axis on rotationally flexible bearings, is considered elsewhere.<sup>5</sup>

### Imperfection sensitivity and minor-axis curvature

6. If a perfect beam is loaded with a uniformly distributed load  $w$ , it will eventually buckle sideways at a load  $w_{cr}$ . When the beam is supported against rotation at its ends, there will also be a variation in twist along the length, as shown in Fig. 2. If the lateral deflection is plotted against load it will follow the curve shown as the perfect case in Fig. 3.

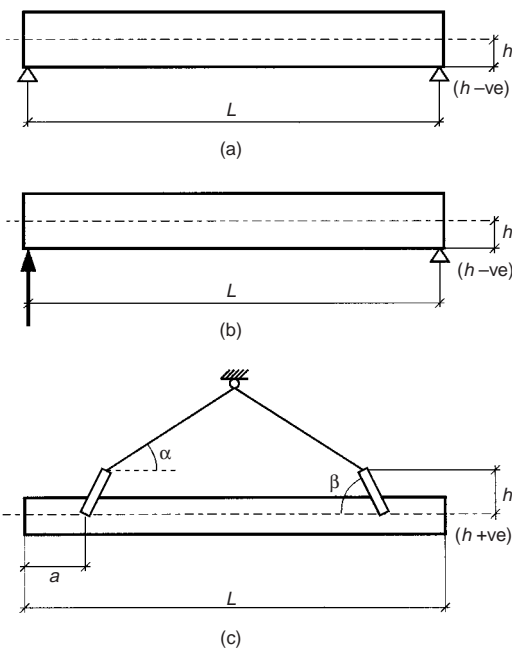


Fig. 1. The three support conditions for beams considered in this paper: (a) simply supported at both ends; (b) supported as for transportation, with the left-hand end supported against displacement, but not rotation; (c) hanging from cables at an angle  $\alpha$ , with yokes at angle  $\beta$  (in practice,  $\beta$  will be either  $\alpha$  or  $90^\circ$ )

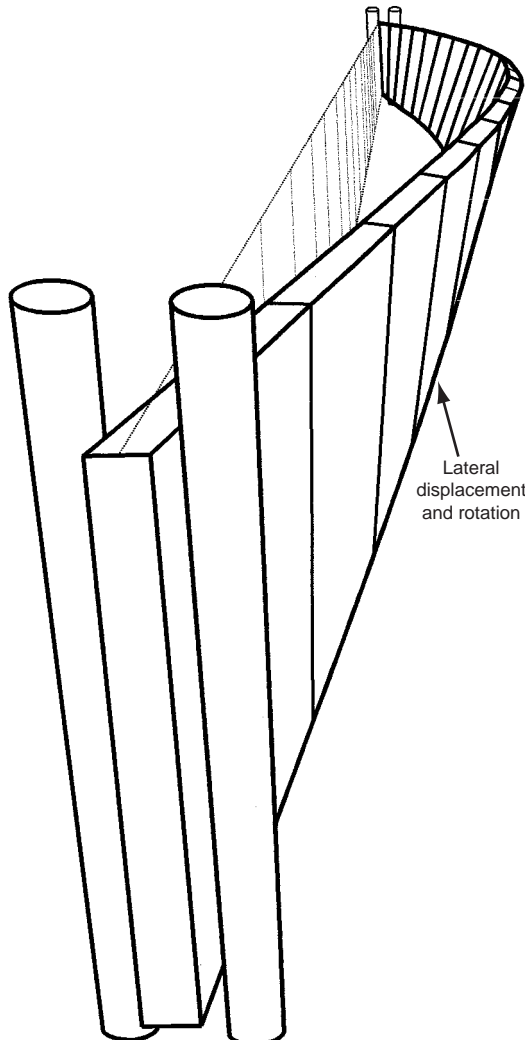


Fig. 2. Idealized view of lateral-torsional buckling mode

The beam will be equally likely to buckle in either direction, and for the problems studied here, the beam will be neutrally stable (meaning that no further increase in load will be possible post-buckling), or will have a stable post-buckling response (which means that the beam can carry a slight increase in load, but at greatly increased lateral deflection).

7. However, no beam is perfect, so the beam will have some lateral deflection before being loaded. In precast prestressed concrete beams, which are normally cast in steel moulds, this imperfection is caused primarily by differences in the forces in the prestressing strands and by variations of the elastic modulus within the concrete. When such a beam is loaded it does not buckle at a fixed load, but the minor-axis deflection tends to increase, eventually becoming asymptotic to the post-buckling response, but only at a large deflection. Similar behaviour occurs if the beam supports are not level.

8. Even if the beam is at a load below  $w_{cr}$ , the lateral deflection can give rise to problems caused by stresses generated by the minor-axis curvature. In cases where the beam is already highly stressed because of the prestress and the dead weight, these can lead to problems, either of overstressing in compression or of cracking of the beam in tension. The tension problem is more serious, since the cracking would tend to reduce further the beam's stiffness, leading to a greater tendency to buckle.

9. There are four distinct quantities that have to be found for each of the loading cases identified above:

- (a) the critical load of a perfect beam
- (b) the load-deflection curve of the imperfect beam
- (c) the curvature associated with a given lateral deflection
- (d) the bending stresses which are additional to those due to the primary bending moment and the prestress.

Fortunately, the same techniques can be used in all cases.

### The Southwell plot

10. A Southwell plot can be used to represent the load-deflection behaviour of a beam that is approaching its buckling load. Southwell<sup>6</sup> showed that plotting deflection/load against deflection for the neutrally stable buckling problem of an axially loaded strut gives a line which becomes asymptotic to a straight line. This line has a gradient of  $1/(w_{cr})$  and an intercept on the deflection axis of  $-v_0$ , where  $v_0$  is the component of the initial imperfection in the buckling mode, as shown in Fig. 4. It should be noted that the deflection that has to be plotted is the one measured from the initial position of the *imperfect* beam

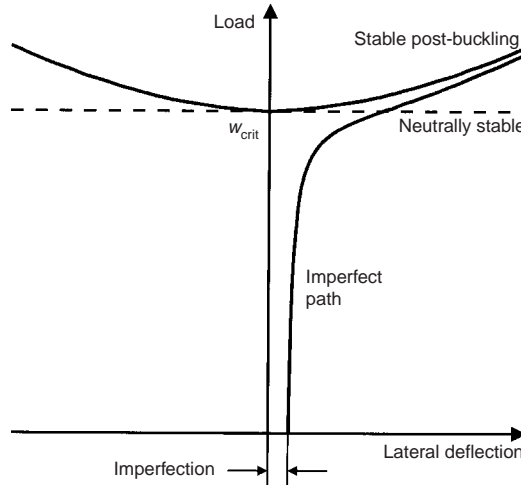


Fig. 3. Fundamental path of stable post-buckling behaviour, and behaviour of imperfect element

$(v - v_0)$ , and not that measured from the axis of the *perfect* beam ( $v$ ).

11. The Southwell construction can also be used in reverse to predict the load-deflection behaviour of a neutrally stable buckling problem, given only values of the critical load and the magnitude of the initial imperfection, as shown in Fig. 4(b). The deflection  $v$  due to a given self-weight  $w$  can be obtained from

$$v = \frac{v_0}{1 - w/w_{cr}} \quad (1)$$

The magnitude of the initial imperfection can be obtained by measurement of existing beams (or a limiting value could be set in a specification). If  $w_{cr}$  is known, the value of the minor-axis deflection can be obtained from equation (1) for any given load  $w$ .

12. Equation (1) applies when the buckling mode involves minor-axis deflections only (as with the toppling of the hanging beam). When the buckling mode involves both minor-axis deflection and torsion (as with lateral-torsional buckling), the relevant form of the Southwell construction<sup>7</sup> is

$$y = \frac{y_0}{1 - (w/w_{cr})^2} \quad (2)$$

The value of  $y_0$  should be the component of the initial deflection in the buckling mode, which is

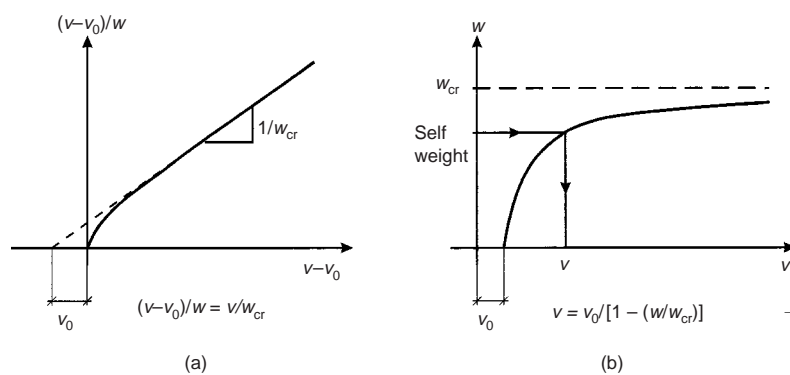


Fig. 4. (a) Southwell plot showing linear behaviour as the load approaches its critical value; (b) corresponding load-deflection plot

very difficult to determine, and the equation strictly only applies to beams which are neutrally stable. However, it was shown<sup>1,2</sup> that the lateral deflection that results from the use of equation (1) or (2) is usually conservative, in that it overestimates the true deflection, so curvatures and stresses which are determined from it will be larger than those which will actually occur. It thus gives a suitable basis for the calculation of the additional stresses that are caused. Cases where this is not true will be pointed out below.

### Assumptions

13. In the previous papers<sup>1,2</sup> critical loads were determined for various support conditions using a finite-element eigenvalue analysis, rigorous analysis or Rayleigh–Ritz approximations. It was determined that warping effects are insignificant for typical concrete beam sections (and neglecting restrained warping effects is conservative anyway). Effects due to the difference between the locations of the shear centre and the centroid have been ignored, as have effects due to the major-axis deflection.

### Loading cases

14. The various cases that have been studied are given below. For each case, equations or design charts will be given from which the critical load of the perfect beam, the minor-axis deflection due to imperfections and the minor-axis curvature can be determined. Derivations are not given here, but are referenced.

#### *Simply supported beam*

15. For typical concrete beam sections the non-dimensional buckling load of a simply supported beam<sup>2</sup> agrees with an analysis by Trahair,<sup>8,9</sup> the result of which can be expressed as

$$w_{\text{cr}} = 28.4 \frac{\sqrt{(GJ EI_y)}}{L^3} \quad (3)$$

The buckling load is independent of the support height since axial rotation is restrained over the supports.

16. *Imperfection in the form of minor-axis deflection.* The inclusion of both the minor-axis stiffness and the St Venant's torsional stiffness indicates that this is a lateral–torsional mode, so the relevant form of the Southwell plot is that given by equation (2). This can be used directly to obtain the minor-axis deflection from the initial imperfection (either measured or assumed).

17. Once the minor-axis deflection has been determined, the twist of the beam at midspan can be found from

$$\frac{\delta\theta}{y_{\text{ms}}} = \frac{\pi}{L} \sqrt{\left(\frac{EI_y}{GJ}\right)} \quad (4)$$

and the minor-axis curvature from

$$\kappa_{\text{ms}} = \frac{wL^2 \sin \delta\theta}{8EI_y} \quad (5)$$

18. *Imperfection in the form of rotated supports.* The rotation of the supports in the minor-axis direction causes the beam's weight to act, in part, about an axis which has very much reduced stiffness, which thus causes significant minor-axis deflection, given by

$$y_{\text{ms}} - \delta_0 = \frac{5wL^4 \sin \eta}{384EI_y} \quad (6)$$

where  $\eta$  is the angle of rotation of the support.

19. This, in turn, will cause torsion and hence additional twist, which will increase the component of the load carried about the minor axis. However, for small loads (approximately  $w < w_{\text{cr}}/4$ ) the torsional effects are found to be negligible, and the lateral deflection of the beam is due to the component of the load which acts in the minor-axis direction ( $w \sin \eta$ ). The corresponding curvature is thus given by

$$\kappa_{\text{ms}} = \frac{wL^2 \sin \eta}{8EI_y} \quad (7)$$

This result is unconservative, and it was found that the Southwell plot construction does not adequately deal with this situation, partly because of the difficulty of determining the relevant value of  $\delta_0$ . It is recommended that if  $w > w_{\text{cr}}/4$  a more rigorous analysis should be carried out to determine the effect of support rotation (or more care should be taken that the supports are level).

#### *Transport-supported beam*

20. For the transport-support condition it was found<sup>2</sup> that the non-dimensional buckling load is

$$w_{\text{cr}} = 16.9 \frac{\sqrt{(GJEI_y)}}{L^3} \quad (8)$$

The finite-element analysis showed (and a Rayleigh–Ritz analysis confirmed)<sup>2</sup> this to be independent of the support height  $h$ , despite the fact that an end support on a ball does not prevent rotation. This is also a lateral–torsional mode.

21. *Imperfection in the form of minor-axis deflection.* The inclusion of both the minor-axis stiffness and the St Venant's torsional stiffness indicates that this is a lateral–torsional mode, so the relevant form of the Southwell plot is that given by equation (2). This can be used directly to obtain the minor-axis deflection from the initial imperfection (either measured or assumed).

22. Once the minor-axis deflection has been

determined, the twist of the beam at midspan can be found from

$$\frac{\delta\theta}{y_{ms}} = \frac{1.68}{-0.36L\sqrt{(GJ/EI_y)} - y_b} \quad (9)$$

and the minor-axis curvature from

$$\kappa_{ms} = \frac{wL^2 \sin \delta\theta}{8EI_y} \quad (10)$$

**23. Imperfection in the form of rotated supports.** For a transport-supported beam, the influence of support rotation is the same as for a simply supported beam. A typical camber on highways in the UK is about  $3^\circ$ , but higher rotations, say of  $6^\circ$ , may be expected on site. This is thus more likely to be a governing condition than misplaced bearings.

**24. Imperfection caused by lateral load.** While being transported, the beam can be subjected to inertial loads caused by the vehicle movement, whose magnitudes are very difficult to determine. Their effect will be to cause lateral displacements, which can be determined by assuming that the beam is simply supported for minor-axis bending. These displacements can then be used as initial imperfections to determine whether a stability problem exists.

**25.** An Australian study<sup>10</sup> showed that articulated trucks were regularly subjected to lateral accelerations of up to  $0.25g$ , which is about 80% of the acceleration needed to overturn them. While it may be expected that trucks carrying large precast beams will be driven more carefully, lateral accelerations of about  $0.1g$  may be expected. This is equivalent to putting the truck sideways on a  $6^\circ$  slope.

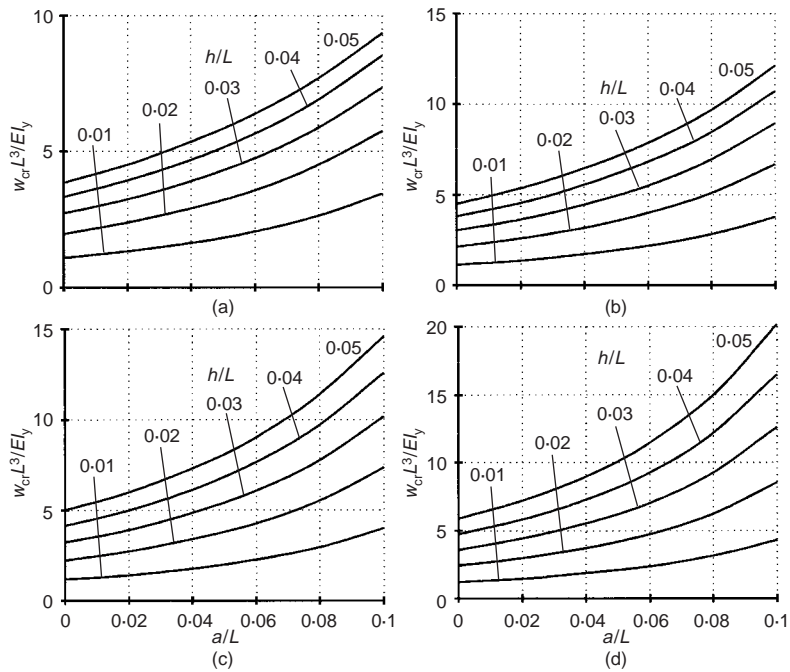
#### Hanging beam

**26.** The finite-element analysis<sup>2</sup> showed that the buckling load of a hanging beam is independent of the torsional stiffness  $GJ$ , and consequently it can be non-dimensionalized using the parameter  $EI_y/L^3$ . This is confirmed by the mode shape which, although it involves a rigid-body rotation, demonstrates only a small variation in twist along the beam.

**27.** An analytical solution was obtained for the hanging-beam problem<sup>1</sup> on the assumption that the beam topples as a rigid body, with only minor-axis deflection. However, the resulting equations have to be solved numerically, so the results are presented here in non-dimensional graphical form.

**28.** Figure 5 shows the variation of non-dimensional buckling load with the geometry of the beam (as shown in Fig. 1). Each plot is for a different value of the cable angle  $\alpha$  and shows curves for different non-dimensional support heights  $h/L$ . These give the variation in buckling load with the non-dimensional attachment position  $a/L$ . (Note the different scales used for the load axis on each plot.)

**29.** The graphs in Fig. 5 show that the



buckling load increases with the support height, as the cables approach vertical, and as the yoke attachment points are moved in from the ends. Owing to the arrangement of prestress in the beam it will not normally be possible to support a beam away from its ends; end support corresponds to the most critical case for buckling.

**30.** Only the case of vertical cables can be reduced to a simple expression:<sup>1</sup>

$$w_{cr} = \frac{12EI_y h}{L^4/10 - aL^3 + 3a^2L^2 - 2a^3L - a^4} \quad (11)$$

This is similar to an equation derived by Mast.<sup>11</sup>

**31. Imperfection sensitivity.** The various general cases of imperfection sensitivity have been considered in detail elsewhere.<sup>1</sup> Only the simplest cases will be considered here.

**32. Inclined cables.** The midspan deflection can be found using the Southwell construction, with the correct initial imperfection:<sup>2</sup>

$$v_{ms} = \frac{\delta_0(1 - \sin \pi a/L)}{(1 - w/w_{cr})} \quad (12)$$

The toppling angle  $\theta$  can be found by substituting the relevant values into

$$\begin{aligned} v_{ms} &= \frac{w \sin \theta}{\mu^4 EI_y} \left[ \left( 1 - \frac{\mu^2 a^2}{2} \right) \right. \\ &\quad \times (\cos \mu b + \tan \mu b \sin \mu b - 1) - \frac{\mu^2 b^2}{2} \left. \right] \\ &\quad + \frac{\pi^2 \delta_0}{\pi^2 - \mu^2 L^2} \\ &\quad \times \left[ 1 - \sin \frac{\pi a}{L} (\cos \mu b + \tan \mu b \sin \mu b) \right] \end{aligned} \quad (13)$$

**Fig. 5. Critical self-weight loads for hanging beams, for vertical yokes ( $\beta = 90^\circ$ ).** The four sets of curves show results for different cable angles  $\alpha$ :  
(a)  $\alpha = 30^\circ$ ;  
(b)  $\alpha = 45^\circ$ ;  
(c)  $\alpha = 60^\circ$ ;  
(d)  $\alpha = 90^\circ$ . The values of  $a/L$  and  $h/L$  correspond to the various support configurations (Fig. 1) (note the different scales on the vertical axes)

where

$$\mu = \sqrt{\left(\frac{wL}{2EI_y} \tan \alpha\right)} \quad (14)$$

and  $b$  is the distance from the yoke attachment point to the centre of the beam ( $L/2 - a$ ). The midspan curvature is then given by

$$\kappa_{ms} = \mu^2 v_{ms} + \frac{w \sin \theta}{2EI_y} (b^2 - a^2) \quad (15)$$

It should be noted that  $v_{ms}$  includes the initial imperfection  $\delta_0$ , but  $\kappa_{ms}$  does not include the initial imperfection curvature  $\kappa_0$ ;  $\kappa_{ms}$  can thus be used directly to give the additional stresses due to lifting.

33. *Vertical cables.* If the cables supporting the beam are vertical, different forms of the equations are required. The midspan deflection is obtained from equation (12) and can then be used to find the rotation  $\theta$  from

$$v_{ms} = \frac{w \sin \theta}{384EI_y} (5L^2 - 20aL - 4a^2)(2a - L)^2 + \delta_0 \left(1 - \sin \frac{\pi a}{L}\right) \quad (16)$$

The midspan curvature is evaluated using

$$\kappa_{ms} = \frac{w \sin \theta}{8EI_y} (L^2 - 4aL) \quad (17)$$

### Determination of minor-axis bending stresses

34. The results of the previous section can be used to determine the critical buckling load  $w_{cr}$  for the particular support condition being studied, and hence the proportion of this that the beam's own weight represents ( $w/w_{cr}$ ). This then leads to the lateral displacement  $v$  caused by a known initial imperfection  $\delta_0$ , and the corresponding additional curvature at midspan  $\kappa_{ms}$  (which again does not include the initial curvature  $\kappa_0$ ). This curvature can be used to determine the stress distribution across the beam; at a distance  $X$  from the beam's major axis the change in the concrete stress  $\Delta\sigma$  can be found from

$$\Delta\sigma = E\kappa_{ms}X \quad (18)$$

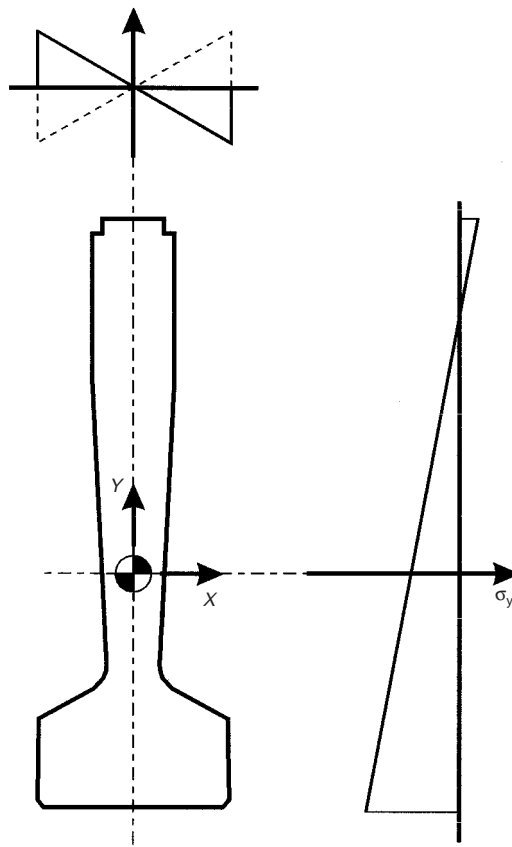
This stress must be superposed on the major-axis stress distribution, allowing the stress at two critical points to be found, as shown in Fig. 6. These critical points will normally be at the corners of the section and will give the largest tensile stresses and the compressive stresses. At these corner points the torsional stresses will be zero; it is not anticipated that torsional stresses elsewhere will be significant and they have not been evaluated in the present study.

35. The value of the minor-axis bending stress will be largest at midspan, and can be expected to reduce to zero at the ends of the beam. The stress distribution that relates to the

### Stress distribution due to bending about the minor axis

Includes stresses due to:

- initial imperfection
  - lateral stability effects ( $\Delta\sigma = E\kappa X$ )
- (sign depends on direction of initial imperfection)



### Stress distribution due to bending about the major axis

Fig. 6. Stresses to be combined when assessing a beam (note that minor-axis stresses can be in either sense)

initial imperfection should also be included here; this paper makes no attempt at evaluating those stresses, since they are heavily dependent on the original cause of the initial imperfection.

36. The major-axis stress distribution  $\sigma_y$  includes the effects of

- self-weight bending moment in the major-axis direction
- the stress distribution due to the prestress
- if the beam is hanging from inclined cables, the additional force and bending moment resulting from the axial force present in the inclined cables.

Designers should satisfy themselves that the appropriate combinations of these stresses are considered when checking the stresses; detailed equations are not given here, since there are many possible combinations.

### The tensile concrete stress limit

37. Mast<sup>12</sup> carried out a lateral bending test on a 45·4 m long prestressed I-beam to investigate its behaviour once cracked. He found that the beam could tolerate lateral loads considerably in excess of the theoretical cracking load

without any visible sign of damage, *once the lateral load was removed*, and presented a method which can be used to predict a typical prestressed beam's behaviour once cracking has started.<sup>13</sup> However, cracking influences the minor-axis stiffness, which has a direct influence on the buckling load. This idea led Swann and Godden<sup>14</sup> to state that if a cracked section is allowed during lifting there will be a reduction in the beam's stiffness, resulting in increased deflection and the potential for a self-propagating failure which would occur without warning. It is thus recommended that a cracked section should not be allowed, although the tensile strength of the concrete may be taken into account if the lifting is carried out under controlled conditions.

### Stiffening frame

38. The use of temporary stiffening frames was considered by Mast,<sup>13</sup> who concluded that they had a relatively minor effect on the buckling load. However, by careful choice of frame geometry, the effect can be enhanced, not only by increasing the critical load, but also by reducing the additional deformation caused by the initial imperfections. An analysis of stiffening frames, using the techniques discussed here, is given elsewhere.<sup>15</sup>

### Sample calculations

39. Results of stability calculations are presented below for four typical precast beams.

#### M-10 beam, 29·5 m long

40. The M-10 beam is the largest beam in the M-beam series,<sup>16</sup> chosen here to show that stability criteria are not particularly significant for beams of this type. It is designed to have a maximum length of 29·5 m, and it is assumed here that the longest beam is supported by yokes that extend 400 mm above the upper surface of the beam when hanging.

#### SY-6 beam, 40 m long

41. The SY series of beams is the largest standard series of precast beams currently manufactured in the UK.<sup>4</sup> They are narrower, deeper, longer and heavier than the M-series beams, and on each count can be expected to be more susceptible to stability problems. The maximum recommended length for these beams is 40 m. It is assumed that these beams, when hanging, are supported from vertical yokes that extend 0·455 m above the top surface ( $h = 1\cdot6$  m).

#### SY-6 beam, 44 m long

42. Results are also presented for SY-6 beams used at lengths beyond that for which they have been designed, to illustrate the way in which a 10% increase in length can have a significant adverse effect on the stability be-

haviour of the beam. In practice, if a longer beam were required, the section would probably be altered. If stability criteria were ignored, the major-axis stiffness would be increased, at the expense of the minor-axis stiffness, in order to keep the weight down, which would exacerbate the tendency to buckle. This example, and indeed these papers, have been published in order to draw attention to that problem.

#### Roof beams, 33·5 m long

43. Lest it be thought that long, thin beams are either new or restricted to bridges, an older example is given. This consists of beams designed by Harris<sup>17</sup> and used to span hangars at London (now Heathrow) Airport in 1951. The beams were of a T-section, 6 ft (1·828 m) deep and 3 ft (0·914 m) wide, with 4 in (102 mm) thick webs and flanges. The beams were 110 ft (33·5 m) long and built from segments, post-tensioned together on the ground, which were then lifted into place with a spreader beam. The analysis here assumes that the beams are supported at their ends at the level of the top surface.

#### Common factors

44. The concrete is assumed to have a Young's modulus of 34 kN/m<sup>2</sup>; Poisson's ratio has been taken as 0·15 in all cases. The level of the initial lateral imperfection has been taken as span/1000, while for rotated supports, a misalignment of 2° is assumed; both of these factors imply good quality control in manufacture and handling. Figure 7 shows comparative cross-sections.

45. Table 1 shows the results of the calculations. The section properties have been taken from published data or calculated by standard methods; junction effects have been taken into account when calculating the torsion constant.<sup>18</sup> The table shows that all the beams have reserves of resistance to lateral torsional buckling while simply supported, their weights ranging from 4% (M-10) to 15% (roof) of their critical loads. Similarly, the stresses due to the

Fig. 7. Comparative sections of M-10 and SY-6 bridge beams and airport roof beams

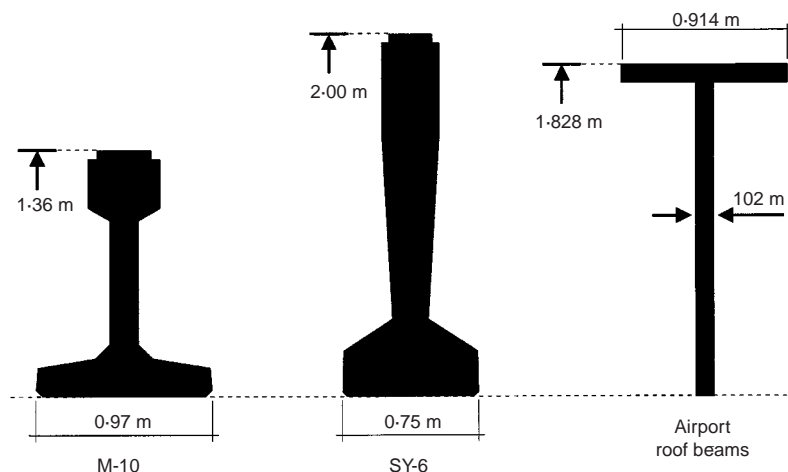


Table 1. Results of stability calculations

	Variable	Units	M-10	SY-6 40 m long	SY-6 44 m long	Hangar roof
Overall beam height	$d$	m	1.36	2	2	1.828
Overall beam width		m	0.97	0.75	0.75	0.914
Height of centroid above soffit	$y_b$	m	0.568	0.855	0.855	1.18
Cross-sectional area	$A$	$\text{m}^2$	0.457	0.709	0.709	0.2684
Second moment of area about major axis	$I_{xx}$	$\text{m}^4$	0.1019	0.2837	0.2837	0.09473
Second moment of area about minor axis	$I_{yy}$	$\text{m}^4$	0.0183	0.014	0.014	0.006642
St Venant's torsion constant	$J$	$\text{m}^4$	0.006	0.0221	0.0221	0.000918
Young's modulus of concrete	$E$	GPa	34	34	34	34
Shear modulus of concrete	$G$	GPa	14.8	14.8	14.8	14.8
Beam weight	$w$	kN/m	10.79	16.73	16.73	6.33
Span/initial imperfection	$L/d_0$		1000	1000	1000	1000
<i>Simply supported analysis</i>						
$w/w(\text{crit})$	$w/w_{\text{cr}}$			0.04	0.10	0.15
Stress due to minor-axis deflection	$\Delta\sigma$	MPa		0.26	0.34	0.42
Stress due to support rotation	$\Delta\sigma$	MPa		1.09	3.13	3.79
<i>Transport-supported beam</i>						
$w/w(\text{crit})$	$w/w_{\text{cr}}$			0.07	0.16	0.21
Stress due to minor-axis deflection	$\Delta\sigma$	MPa		0.34	0.48	0.60
<i>Hanging beam (vertical cables)</i>						
Height of support	$h$	m		1.19	1.6	1.6
Length of overhang	$a$	m		0	0	0
$w/w(\text{crit})$	$w/w_{\text{cr}}$			0.09	0.47	0.69
Minor-axis bending stresses (imperfect)	$\Delta\sigma_0$	MPa		5.52	3.15	2.86
Minor-axis bending stresses (lifting)	$\Delta\sigma_{\text{ms}}$	MPa		0.54	2.70	6.08
						0.648
						0.45
						4.58
						3.71

assumed initial imperfections are all less than 1 MPa. Transport-supported beams also show a reasonable reserve against buckling, and low stresses caused by imperfections. However, the stresses caused by even a small rotation (2°) of the supports is larger, being nearly 4 MPa in the case of the 44 m long SY-beam. (The same stresses will be caused in both the simply supported and the transport-supported case.) These values do not seem high by themselves, but it must be noted that these are magnitudes, and must be added to and subtracted from the stresses that are already present in the beam, and which may have been the limiting factors in the design. Note also that the lateral accelerations to be expected while driving may be equivalent to a 6° slope.

46. When the hanging beam is considered, the situation is worse. The M-10 beam, which is acting at only 9% of its critical load, has additional stresses of only ±0.5 MPa induced when hanging, although the initial imperfection is itself associated with stresses of ±5.5 MPa. For the 40 m long SY-6 beam, additional stresses of ±2.7 MPa occur, with the beam acting at 47% of its buckling load; these are significant, but can be taken into account at the design stage. However, if the span was increased to 44 m, the SY-6 beam would be acting at 69% of the critical load and the additional stresses would increase to

±6.1 MPa, clearly demonstrating the problems that would be induced if these beams were used in this way. The airport roof beams were also operating at 45% of their buckling loads, with stresses as large as ±3.7 MPa being induced.

47. It should be noted that these stresses are caused by bending about the minor axis, so are at their worst at the extreme edges of the widest part of the beam. For the airport roof beams, this was at the top of the section, where the residual prestress would have been lowest. For the precast bridge beams, which are designed to have an *in situ* composite slab added at a later stage, the widest part is at the bottom, where a significant prestress can be expected. Nevertheless, the stresses being predicted here, for relatively small initial imperfections, indicate that some attention should be paid to these stability criteria in future.

48. The additional stresses induced during transportation, lifting and while on temporary supports are only transitory. They will thus not cause creep, and it is resistance to creep effects which normally sets the compressive stress limits for precast beams. In the same way, it may be reasonable to allow some tensile stresses (but less than the modulus of rupture) for purely temporary loadings, provided that the beams are handled in a controlled way. The choice of the limiting criteria for a particular situation must remain with the engineer.

## Buckling of cambered beams

49. A typical prestressed concrete beam will be cambered, which raises the centre of gravity of the beam. No account of this has been taken in this paper. Peart, Rhomberg and James<sup>19</sup> found that, for beams lifted using vertical cables, camber gives a significant reduction in the beam's buckling load, particularly for long beams with large amounts of camber. Some allowance can be made for this effect by reducing the value of  $h$  by the amount of the camber when calculating the critical load. The result will not be exact and will only be reasonable if the yokes are rigidly attached to the beam.

## Recommendations for handling long concrete beams

50. It is possible to make some simple recommendations to minimize the risk of failure during lifting, transportation and erection.

### Lifting

51. The cables should be as near vertical as possible. This could be implemented by using a spreader beam, although the additional weight of this should be considered when assessing crane capacity.

52. The length of the lifting yoke should be increased to give an increase in support height.

53. The yoke attachment positions should be brought in from the ends of the beam. The optimum position is somewhere near the beam's quarter points, but owing to the prestress design of the beam it is unlikely that this arrangement could be used.

54. Prestress design should take into account the extra stresses present during lifting due to lateral self-weight loading and additional lateral loads, since these can be very significant.

55. Lateral imperfections should be kept to a minimum. A small lateral bow will always be present because of the manufacturing process. However, lateral misplacement of the lifting yokes and cables could also introduce significant imperfections. The yokes should be designed so that they fit centrally onto the beam and that the cable in turn fits centrally onto the yoke, with no possibility of slipping. The yokes should also be made as laterally stiff as possible.

### Transportation

56. During transportation, lateral loads due to tilting of the beam, wind loading and dynamic effects are important. The magnitudes of the forces to which a beam is likely to be subject are difficult to assess.

57. Excessive tilt due to road superelevation or while manoeuvring on site should be avoided.

58. Both for lifting and during transportation, temporary post-tensioning may be used to

reduce the tensile stresses within the beam, as suggested by Laszlo and Imper,<sup>20</sup> if adequate reserves against stability problems cannot otherwise be provided.

## Conclusions

59. This paper has investigated potential problems that may arise when handling increasingly long and slender modern precast concrete beams. It has described how buckling instability can lead to failure and has highlighted the most susceptible support conditions.

60. Once the beam is in its final position the beam's self-weight is much less than its buckling load so that buckling failure is unlikely. However, care should be taken to ensure the supports are level.

61. During transportation a perfectly straight beam is also unlikely to buckle, but lateral loading due to road superelevation, wind loading and dynamic effects cause significant stress in the concrete and could lead to failure.

62. Beams are most susceptible to buckling during lifting. A method for assessing the stability of hanging beams has been presented, and this has shown that modern 40 m long SY-6 beams are considerably more likely to buckle than older M-10 beams. The presence of initial imperfections in the beam can cause large stresses in the concrete which can now be assessed.

63. This paper has shown that a beam is more likely to fail as its length increases. Future developments which increase the length of precast beams are likely to make the beams more susceptible to buckling failure.

## References

- STRATFORD T. J. and BURGOYNE C. J. The toppling of hanging beams. *International Journal of Solids and Structures*, in press.
- STRATFORD T. J. and BURGOYNE C. J. Lateral stability of long precast concrete beams. *Proceedings of the Institution of Civil Engineers: Structures and Buildings*, 1999, **124**, 169–180.
- TAYLOR H. P. J., CLARK L. A. and BANKS C. C. The Y-beam: a replacement for the M-beam in beam and slab bridges. *The Structural Engineer*, 1990, **68**, 459–465.
- PRESTRESSED CONCRETE ASSOCIATION. *Data Sheet for SY-beams*. Prestressed Concrete Association, Leicester, 1995.
- BURGOYNE C. J. and STRATFORD T. J. Buckling of heavy beams on rotationally flexible bearings. In preparation.
- SOUTHWELL R. V. On the analysis of experimental observations in problems of elastic stability. *Proceedings of the Royal Society, Series A*, 1932, **135**, 601–616.
- ALLEN H. G. and BULSON P. S. *Background to Buckling*. McGraw-Hill, London, 1980.
- TRAHAIR N. S. *The Behaviour and Design of Steel Structures*. Chapman and Hall, London, 1977.
- TRAHAIR N. S. *Flexural-Torsional Buckling of Structures*. E. & F. N. Spon, London, 1993.

10. GEORGE R. M. Behaviour of articulated vehicles on curves. *Third International Symposium on Heavy Vehicle Weights and Dimensions* (eds D. Cebon and C. G. B. Mitchell). Thomas Telford, London, 1992.
11. MAST R. F. Lateral stability of long prestressed concrete beams, part 1. *PCI Journal*, 1989, **34**, 34–53.
12. MAST R. F. Lateral bending test to destruction of a 149 ft prestressed concrete I-beam. *PCI Journal*, 1994, **39**, 54–62.
13. MAST R. F. Lateral stability of long prestressed concrete beams, part 2. *PCI Journal*, 1993, **38**, 70–88.
14. SWANN R. A. and GODDEN W. G. The lateral buckling of concrete beams lifted by cables. *The Structural Engineer*, 1966, **44**, No. 1, 21–33.
15. BURGOYNE C. J., STRATFORD T. J. and TAYLOR H. P. J. The use of stiffening frames with precast concrete beams. In preparation.
16. MANTON B. H. and WILSON C. B. *MoT/C&CA Standard Bridge Beams, Prestressed Inverted T-beams for Spans from 15 m to 29 m*. Cement and Concrete Association, London, 1971.
17. HARRIS A. J. Hangars at London Airport, design of large span prestressed concrete beams. *The Structural Engineer*, 1952, **30**, 226–235.
18. BURGOYNE C. J. Junction effects in St Venant's torsional stiffness. *The Structural Engineer*, 1993, **71**, No. 3, 47–53.
19. PEART W. L., RHOMBERG E. J. and JAMES R. W. Buckling of suspended cambered girders. *ASCE Journal of Structural Engineering*, 1992, **118**, No. 2, 505–528.
20. LASLO G. and IMPER R. R. Handling and shipping of long-span bridge beams. *PCI Journal*, 1987, **32**, 86–101.

**Please email, fax or post your discussion contributions to the publisher: email: ttjournals@ice.org.uk; Fax: 0171 538 9620; or post to Terri Harding, Journals Department, Thomas Telford Limited, Thomas Telford House, 1 Heron Quay, London E14 4JD.**